Standard-Compliant Jitter Transfer Function of All-Optical Clock Recovery at 40 GHz Based on a Quantum-Dot Self-Pulsating Semiconductor Laser

J. Renaudier, B. Lavigne, F. Lelarge, M. Jourdran, B. Dagens, O. Legouezigou, P. Gallion, and G.-H. Duan

***Abstract*—This letter reports on all-optical clock recovery over 40-Gb/s signal using a quantum-dot (QD)-based self-pulsating (SP) laser. In particular, the jitter transfer function from the input signal to the recovered clock is measured for the first time. We clearly demonstrate that, thanks to the narrow spectral linewidth of the free-running SP signal, the QD-based laser allows the suppression of high frequency jitter, and the cutoff frequency is exactly that required by the ITU-T recommendation G825.1 at 40 GHz.**

***Index Terms*—Clock recovery, self-pulsation, semiconductor lasers.**

I. Introduction

In order to improve transmission distance, capacity, and speed of optical networks, much attention has been paid to investigate a practical means for all-optical signal processing, such as all-optical digital logic functions or 3R regenerators [1], [2]. One solution to achieve the regeneration is the combination of a Mach–Zehnder interferometer with an all-optical clock recovery [2], [3]. Among the different approaches investigated so far to accomplish all-optical clock recovery, self-pulsating (SP) semiconductor lasers are attractive structures because they are expected to synchronize their own SP frequency to the clock component of a return-to-zero (RZ) incoming data signal [4]. Unlike RZ data, nonreturn-to-zero (NRZ) data do not contain any clock component. However, preprocessing methods have been developed to extract optically a clock component from NRZ data [5], [6] allowing the use of SP lasers for all-optical clock recovery. In this respect, SP semiconductor lasers based on bulk or quantum-well structures have shown interesting results at high bit rates [7]–[10]. Nevertheless, little information has been given on the jitter characteristics of the recovered clocks. The compliance of the jitter filtering functions with ITU-T standards for clock recovery schemes is mandatory for practical applications of all-optical clock recovery.

Recently, SP laser diodes based on quantum-dot (QD) structures are attracting much attention as they provide RF oscillators with fast carrier dynamics and much better spectral purity [11], [12]. Such properties are of great interest for the realization of all-optical clock recoveries with an efficient jitter filtering function. In this letter, we report phase noise (PN) measurements on a 40-GHz clock recovery made on an SP QD Fabry–Pérot (FP) laser. We demonstrate for the first time to our knowledge, that such a QD-based laser enables a high frequency jitter suppression that meets the ITU-T recommendation G825.1 requirements thanks to its intrinsic narrow free running spectral linewidth, as compared with lasers made on bulk or quantum wells.

Manuscript received December 20, 2005; revised February 24, 2006. This work was conducted in the framework of the French RNRT project "ROTOR."

J. Renaudier is with the Alcatel-Thales III-V Laboratory, 91460 Marcoussis, France. He is also with the Département Communications et Electronique, Ecole Nationale, Supérieure des Télécommunications, 75634 Paris, Cedex 13, France.

B. Lavigne is with Alcatel Research & Innovation, 91460 Marcoussis, France.

F. Lelarge, B. Dagens, O. Legouezigou, and G.-H. Duan are with the Alcatel-Thales III-V Laboratory, 91460 Marcoussis, France.

M. Jourdran is with Aeroflex Europtest, 78990 Elancourt, France.

P. Gallion is with the Département Communications et Electronique, Ecole Nationale, Supérieure des Télécommunications, 75634 Paris, Cedex 13, France.

Digital Object Identifier 10.1109/LPT.2006.875338

II. Component and Setup Descriptions

The SP laser under study is an FP-type semiconductor laser, with a buried ridge structure and a QD-based active layer on InP (100) substrate. More precisely, the active core is made with six layers of InAs QD enclosed within 40-nm-thick barriers and two 40-nm-thick separate confinement heterostructure (SCH) layers ($\lambda_g = 1.17$ μm). The density of dots per QD layer is about 2.10^{10} cm^{-2}, and the typical thickness and width of QDs are 2.3 nm and 20–40 nm (see [13] for details). The studied component is a 1080-μm-long FP laser with both facets cleaved. It is worth noting here that the cavity structure should not have any impact on the clock recovery performance in terms of jitter characteristics. The QD-FP laser has a central lasing wavelength around 1500 nm and self-pulsates around 39.4 GHz with a free running spectral linewidth measured around 20 kHz with the help of an electrical spectrum analyzer after photodetection.

We display in Fig. 1 the experimental setup used to test this component in a 40-GHz optical clock recovery scheme. In order to control the amount of jitter of the incoming data signal at 40 Gb/s, a pattern generator is synchronized by a 10-GHz external clock provided by a synthetizer, the jitter of which is monitored by a white noise generator in the range 10 kHz–1 GHz, provided by a Europtest jitter analyzer. Thus, the pattern generator provides both a clock signal at 10 GHz and a pseudorandom sequence (PRBS) at 10 Gb/s, the amounts of jitter of which can be modified. The two signals delivered by the pattern generator drive, respectively, a gain-switched laser (lasing at 1552 nm) and a $LiNbO_3$ modulator. The modulated signal is then launched into an optical time-division multiplexer (OTDM) that delivers the 40-Gb/s signal. When no PRBS data drive the external modulator, OTDM delivers a 40-GHz optical clock that will be considered later on as the reference clock (ref-ck). A polarization controller is added due to the polarization sensitivity of the QD active layer of the FP laser. The recovered clock signal is then amplified by a semiconductor optical am-

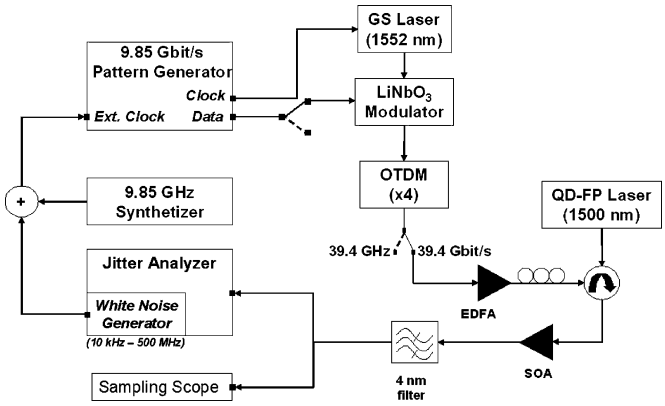

Fig. 1. Experimental setup for clock recovery at 39.4 GHz.

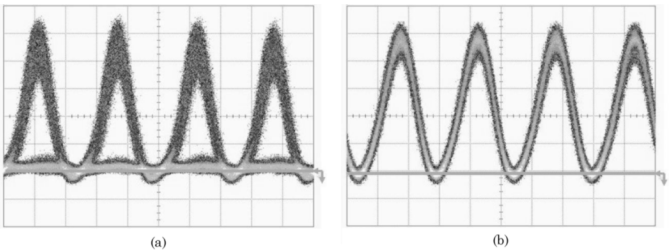

Fig. 2. (a) Eye diagram of the incoming unjittered $2^{31}-1$ OTDM signal, and (b) the corresponding recovered clock. The temporal scale is 10 ps/div.

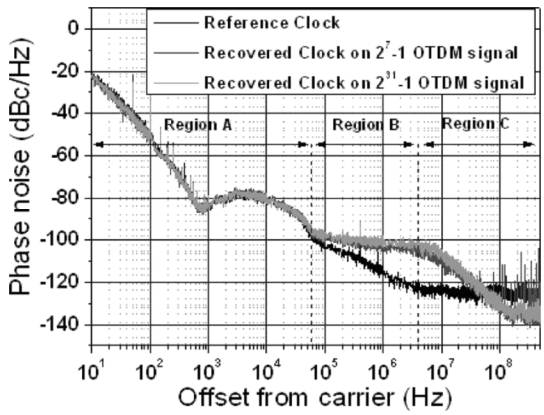

Fig. 3. PN measurements performed on the unjittered reference clock (lower curve) and on the QD-FP laser recovered clocks.

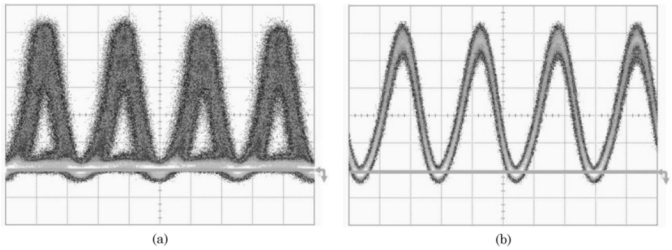

Fig. 4. (a) Eye diagram of the incoming jittered $2^{31}-1$ OTDM signal, and (b) the corresponding recovered clock. The temporal scale is 10 ps/div.

plifier and filtered by a 4-nm bandwidth optical filter before being analyzed either on a sampling scope or on a jitter analyzer. The jitter analyzer provides PN spectra from which we deduce with high accuracy the root-mean-square (rms) jitter in the bandwidth 100 Hz–500 MHz. In this study, the QD-FP laser is biased with a dc current of 210 mA and locked at 39.4 GHz. Besides, a launched optical power of 8 dBm is required partly due to the high coupling loss of the chip test-bench and also because the input signal wavelength is rather far from the gain spectrum of the QD-FP laser. With a reduced detuning between the gain peak and the input signal wavelength, one can expect to decrease the injection power below 3 dBm. For 8 dBm of input power, we measure a locking bandwidth of 6 MHz, which is related to the narrow free running spectral linewidth of some tens of kilohertz [12], [14]. In comparison, the spectral linewidth is typically in the range of several hundreds of kilohertz and several megahertz with quantum wells [15] and bulk, respectively [16].

III. QD-Laser-Based Optical Clock Recovery

A. Locking on Unjittered OTDM Signal

As first evaluation, we analyzed the quality of the recovered clock emitted at 1500 nm by the QD-FP laser with respect to the PRBS length of the incoming OTDM signal without any addition of jitter. As an example, Fig. 2(a) shows a temporal trace recorded when using a $2^{31}-1$ PRBS as incoming signal. As may be seen on Fig. 2(b), we observe a high-quality recovered clock signal with sinus shape and high extinction ratio (estimated to exceed 13 dB). To get more information on the jitter characteristics of this clock recovery scheme, we have measured the PN spectra of the recovered clocks obtained with different PRBS lengths of the incoming OTDM signal. Fig. 3 displays PN curves recorded with a PRBS length varying from 2^7-1 to $2^{31}-1$. As a reference curve, the PN curve of the reference clock (ref-ck) is also reported. Spurious spikes appearing on QD-FP laser PN curves for frequencies higher than 50 MHz originate from PRBS contributions (2^7-1). QD-FP laser PN curves can be split up into three regions as described in [17]. In the frequency region below 60 kHz (A), the noise is dominated by the incoming signal and the clock recovery is fully transparent, i.e., there is no jitter filtering effect. Conversely, for frequencies higher than 4 MHz (Region C), we observe a clear demonstration of a jitter filtering effect with a $1/f^2$ slope (-20 dB/decade): the noise is then determined by the QD-FP laser. The frequency range extending from 60 kHz to 4 MHz (Region B) corresponds to the transition region where the noises from the incoming signal and the laser itself contribute both. The calculated rms jitter varies from 0.16 (ref-ck) to 0.198 ps (with OTDM $2^{31}-1$). Moreover, there is no difference on the laser PN spectra whatever the ODTM PRBS length, attesting of the quality of the recovered clocks.

B. Locking on Jittered OTDM Signal

The jitter removal can be more clearly demonstrated by now injecting a jittered signal into the QD-FP laser. In this respect, we use the white noise generator to add jitter to the reference clock, and consequently, to the incoming OTDM signal. Fig. 4(a) and (b) gives, respectively, the eye diagram of the incoming jittered $2^{31}-1$ OTDM signal, and the corresponding recovered clock from the QD-FP laser, showing a drastic decrease of the time jitter. Again, to get more insight to this phenomenon, Fig. 5 shows the measured PN spectra of the recovered clocks obtained with different PRBS lengths of the jittered incoming OTDM signal, as well as the PN spectrum of the corresponding jittered reference clock. The comparison

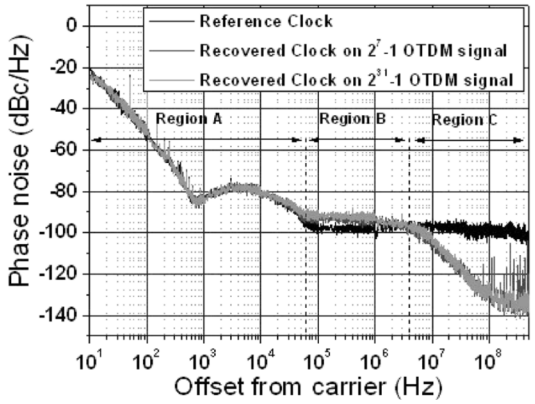

Fig. 5. PN measurements performed on the jittered reference clock (upper curve) and on the QD-FP laser recovered clocks.

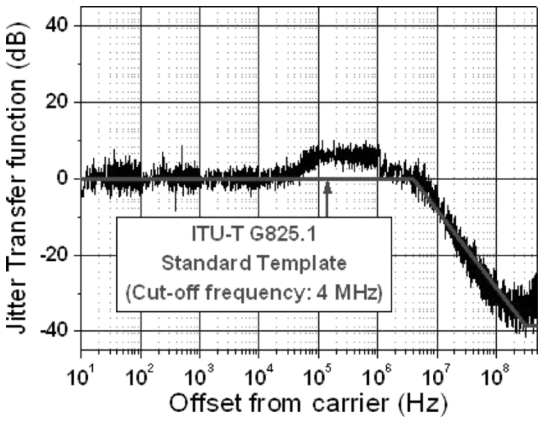

Fig. 6. Measured JTF and comparison with ITU-T G825.1 template.

between the PN spectra of the recovered clock with that of the jittered reference clock clearly explains the drastic decrease of time jitter observed on the sampling scope through the filtering effect operated by the QD-FP laser. Hence, the calculation of the rms jitter from the PN measurements shows a reduction from 1.37 ps for the input to 0.31 ps for the recovered clock in the worst case (PRBS of $2^{31} - 1$). These results undoubtedly demonstrate the efficiency of high-frequency jitter suppression operated by the QD-FP laser, whatever the OTDM PRBS length.

IV. Jitter Transfer Function

As another clear illustration of the jitter removal, we report for the first time to our knowledge the jitter transfer function (JTF) of an all-optical clock recovery. This curve in decibels, given by Fig. 6, is obtained from Fig. 5 by simply subtracting the PN spectrum of the jittered reference clock to the one of the QD-FP laser when the incoming signal is the jittered reference clock itself. The JTF template expected from ITU-T recommendation G825.21 for clock recovery schemes is also plotted on this figure. As one can see, we obtain a very good agreement between the measured JTF from the QD-FP laser and the JTF template expected from ITU-T recommendation G825.21. It is to be noticed that, currently, such a JTF can only be achieved with a QD laser thanks to its narrow free running spectral linewidth.

V. Conclusion

We have shown in this letter an all-optical clock recovery over 40-Gb/s signal based on a QD-FP SP laser. From PN measurements, we clearly demonstrate that the QD-based laser realizes a high-frequency jitter suppression, as expected from a clock recovery. In addition, we present for the first time to our knowledge a JTF measured on an all-optical device, and its very good agreement with the ITU-T recommendation G825.1, showing the potential of this all-optical device to meet the requirements defined for electronic devices. Such a result constitutes a new step toward practical applications of SP semiconductor lasers for all-optical clock recovery at 40 GHz.

References

[1] A. Jourdan, "The perspective of optical packet switching in IP dominant backbone and metropolitan networks," *IEEE Commun. Mag.*, vol. 39, no. 3, pp. 136–141, Mar. 2001.

[2] B. Lavigne *et al.*, "Cascade of 100 optical 3R regenerators at 40 Gbit/s based on all-active Mach–Zehnder interferometer," in *Proc. Eur. Conf. Optical Communications (ECOC)*, 2001, Paper We.F.2.6.

[3] ——, "Test at 10 Gbit/s of an optical 3R regenerator using an integrated all-optical clock recovery," in *Proc. Eur. Conf. Optical Communications (ECOC)*, vol. II, 1999, pp. 262–263.

[4] B. Sartorius *et al.*, "All-optical clock recovery module based on self-pulsating DFB laser," *Electron. Lett.*, vol. 34, no. 17, pp. 1664–1665, 1998.

[5] H. J. Lee *et al.*, "All-optical clock recovery from NRZ data with simple NRZ-to-PRZ converter based on self-phase modulation of semiconductor optical amplifier," *Electron. Lett.*, vol. 35, pp. 989–990, 1999.

[6] W. Mao *et al.*, "All-optical enhancement of clock and clock-to-data suppression ratio of NRZ data," *IEEE Photon. Technol. Lett.*, vol. 13, no. 3, pp. 239–241, Mar. 2001.

[7] C. Bornholdt *et al.*, "Self-pulsating DFB laser for all-optical clock recovery at 40 Gbit/s," *Electron. Lett.*, vol. 36, no. 4, pp. 327–328, 2000.

[8] T. Ohno *et al.*, "Recovery of 40 GHz optical clock from 160 Gbit/s data using regeneratively modelocked semiconductor laser," *Electron. Lett.*, vol. 39, no. 5, pp. 453–455, 2003.

[9] Y. Li *et al.*, "Wavelength and polarization insensitive all-optical clock recovery from 96-Gb/s data by using a two-section gain-coupled DFB laser," *IEEE Photon. Technol. Lett.*, vol. 15, no. 4, pp. 590–592, Apr. 2003.

[10] G.-H. Duan *et al.*, "40 GHz all-optical clock recovery using polarization insensitive distributed Bragg reflector lasers," in *Proc. Conf. Lasers and Electro-Optics (CLEO)*, Baltimore, MD, 2003, Paper CThQ5.

[11] T. Akiyama *et al.*, "Quantum dots for semiconductor optical amplifiers," in *Proc. Optical Fiber Communication Conf. (OFC)*, Anaheim, CA, 2005, Paper OWM2.

[12] J. Renaudier *et al.*, "45 GHz self-pulsation with narrow linewidth in quantum dot Fabry–Pérot semiconductor lasers at 1.5 μm," *Electron. Lett.*, vol. 41, no. 18, pp. 1007–1008, 2005.

[13] F. Lelarge *et al.*, "Room temperature continuous-wave operation of buried ridge stripe lasers using InAs-InP (100) quantum dots as active core," *IEEE Photon. Technol. Lett.*, vol. 17, no. 7, pp. 1369–1371, Jul. 2005.

[14] G.-H. Duan *et al.*, "Injection locking properties of self-pulsation in semiconductor lasers," *Proc. Inst. Elect. Eng., Optoelectronics*, vol. 144, no. 4, pp. 228–233, Aug. 1997.

[15] K. Sato, "Optical pulse generation using Fabry–Pérot lasers under continuous-wave operation," *IEEE J. Sel. Topics Quantum Electron.*, vol. 9, no. 5, pp. 1288–1293, Sep./Oct. 2003.

[16] J. Renaudier *et al.*, "Polarization insensitive 40 GHz self-pulsating DBR lasers with wide self-pulsation frequency tunability," in *Proc. Conf. Lasers and Electro-Optics (CLEO)*, Baltimore, MD, 2005, Paper CtuV5.

[17] O. Brox *et al.*, "Timing stability of injection-locked 40 GHz self-pulsating DFB-lasers," in *Proc. Eur. Conf. Optical Communications (ECOC)*, Anaheim, CA, 2003, Paper Tu4.5.3.